J Solid State Electrochem (2012) 16:2121–2126
DOI 10.1007/s10008-011-1626-y

ORIGINAL PAPER

Formation of two-dimensional (2D) lead dendrites by application of different regimes of electrolysis

Nebojša D. Nikolić · Goran Branković · Uroš Č. Lačnjevac

Received: 21 September 2011 / Revised: 30 November 2011 / Accepted: 11 December 2011 / Published online: 30 December 2011

Abstract Electrodeposition of lead from nitrate electrolyte in constant regimes of electrolysis was analyzed and the obtained powder lead deposits were examined by scanning electron microscopy. Polarization curve for lead electrodeposition consisted of two parts separated by an inflection point. The first part of the polarization curve was characterized by a linear dependence of the current density on overpotential. The linear part of the polarization curve corresponded to ohmic-controlled electrodeposition and single lead crystals were formed in this range of overpotentials. A rapid increase in the current density with increasing overpotential was observed after the inflection point (the second part of the polarization curve). Two-dimensional dendrites were the dominant morphological forms obtained at overpotentials and current densities belonging to the second part of the polarization curve, indicating that the rapid increase of the current density with increasing overpotential corresponded to activation controlled electrodeposition at the tips of the formed dendrites. Comparing the morphologies of the obtained lead deposits with those belonging to the same group of metals (metals characterized by a high exchange current density), such as silver, cadmium, and tin, a strong dependence between the nucleation type and the shape of dendrites for the metals belonging to the same group was established.

N. D. Nikolić (✉)
ICTM-Institute of Electrochemistry,
University of Belgrade,
Njegoševa 12,
11001 Belgrade, Serbia
e-mail: nnikolic@tmf.bg.ac.rs

G. Branković · U. Č. Lačnjevac
Institute for Multidisciplinary Research,
University of Belgrade,
Kneza Višeslava 1a,
11030 Belgrade, Serbia

Keywords Electrodeposition · Lead · Powder · Dendrites · Scanning electron microscope (SEM)

Introduction

Lead is a very important metal from both the academic and practical point of view. The most important technologies of significance for the practical application of lead are the production of high purity active material for acid batteries [1], for semiconductors [2, 3], and in the fabrication of electrochromic devices [4]. Lead in the form of powder has found multiple applications in many industries including oil and gas exploration, radiological medical protective clothing, as an industrial X-ray shield, golf club manufacture, and anti-friction products (http://www.nuclead.com/leadpowderapps.html). In addition, powdered lead is used in lubricating grease to reduce or eliminate wear and as the basis for some corrosion-resistant paints.

The processes of electrochemical deposition are very suitable ways for obtaining lead deposits of the desired form and characteristics for the above-listed applications. They are attained by the choice of the electrolysis regime, the composition of electrolyte solution and the working conditions. The most used electrolytes for lead electrodeposition are acid ones based on chloride [5, 6], bromide [7], iodide [7], nitrate [4, 8], fluorborate [9], acetate [10], fluorosilicate [11–14], etc. Besides acid electrolytes, alkaline solutions are also widely used in lead electrodeposition processes [15, 16]. In the optimization of electrolytes for use in lead battery technology and lead scrap recycling, the effects of some organic additives, such as sorbitol [17] and glycerol [15], were studied. Bright, smooth, and compact lead deposits can be formed by electrodeposition from an acetate bath with the addition of phenol, ethanol, and gelatin as additives [18]. Otherwise, the deposited lead obtained from

an acetate bath without additives was crystalline and showed a marked tendency to form dendrites [10]. Lead powder can be produced from an alkaline solution in the presence of glycerol and it was shown that this additive favors anode dissolution of the powder [19]. The effect of periodically changing regimes of electrolysis, such as pulsating overpotential [10] and reversing current [20], on the formation of lead powder was also examined. Open porous structures, denoted as the honeycomb-like ones, can be formed by electrochemical deposition of lead in the hydrogen co-deposition range [21].

The processes of lead electrodeposition from the basic solutions, such as nitrate ones, are characterized by a high exchange current density [22]. This characteristic of nitrate solutions is of high technological significance because it enables the formation of lead powders at low overpotentials and hence with small spent energy. For this reason, the aim of this study was to examine the production of lead powder from this electrolyte using constant electrolysis regimes. Special attention was given to the examination of the morphology of the attained powder deposits.

Experimental

Lead was electrodeposited from solution containing 0.50 M $Pb(NO_3)_2$ in 2.0 M $NaNO_3$ (pH=3) in an open cell at the room temperature. Doubly distilled water and analytical grade chemicals were used for the preparation of the solutions for electrodeposition of lead.

In the potentiostatic regime, electrodeposition was performed at overpotentials of 50, 100, and 150 mV. In the galvanostatic regime, electrodeposition was performed at current densities of 100 and 160 mA/cm^2. All electrodepositions were performed on vertical cylindrical copper electrodes. The geometric surface area of copper electrodes was 0.25 cm^2.

Reference and counter electrodes were of pure lead. The counter electrode was lead foil with 0.80 dm^2 surface area and placed close to the cell walls. The reference electrode was wire of lead whose tips were positioned at a distance of about 0.2 cm from the surface of the working electrodes. The working electrodes were placed in the center of cell, at the same location for each experiment. The obtained lead deposits were examined using a scanning electron microscope—TESCAN Digital Microscopy.

Results and discussion

Electrodeposition of lead belongs to the fast electrochemical processes because it is characterized by a large exchange current density, i_0 [22]. The polarization curve for lead electrodeposition from a solution containing 0.50 M Pb $(NO_3)_2$ in 2.0 M $NaNO_3$ is shown in Fig. 1. The polarization curve obtained from this solution consists of two parts. The first part is characterized by a linear dependence of the current density on the overpotential. Above an overpotential of about 100 mV, the current density increased quickly, and this rapid increase of the current with overpotential characterizes the second part of the polarization curve.

The linear dependence of the current density on overpotential corresponds to an ohmic-controlled electrodeposition [23, 24]. For sufficiently fast electrode processes ($i_0/i_L \geq 100$), there is no activation or diffusion polarization before the limiting diffusion current density, i_L, is reached. Hence, at current densities lower than the limiting diffusion one, the measured overpotential is due to the ohmic voltage drop between the electrode and the tip of the Lugin capillary [25]. When the limiting diffusion current density is attained, the electrochemical deposition process is under complete diffusion control. However, as seen from Fig. 1, an inflection point on the polarization curve was observed instead of the plateau of the limiting diffusion current density. This inflection point on the polarization curve corresponds to an overpotential of about 100 mV. A survey of the lead surface morphologies obtained at the different overpotentials was considered the most suitable way to analyze this polarization curve and hence, the lead electrodeposition system.

The curves of the dependencies of the current density on electrolysis time obtained at overpotentials of 50, 100, and 150 mV are shown in Fig. 2. A small increase of the current with time was observed during electrodeposition at an overpotential of 50 mV. On the other hand, the current increased rapidly during electrodeposition at overpotentials of 100 and 150 mV. The increase of the current with electrolysis time was faster at 150 mV than at 100 mV. The morphologies of lead deposits obtained under ohmic-controlled deposition, in the transitional zone corresponding to the end of ohmic-

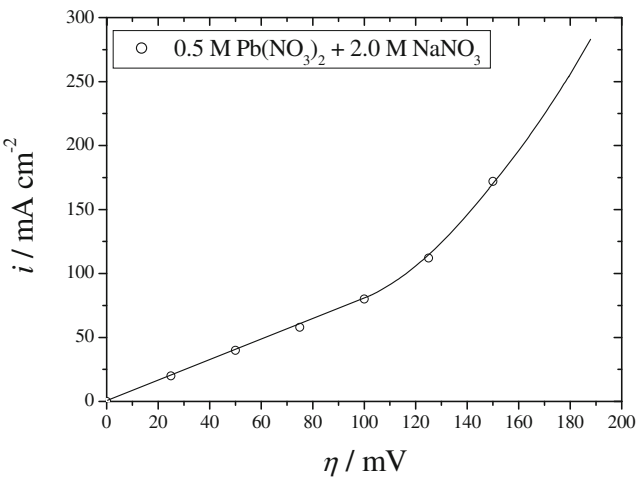

Fig. 1 Polarization curve for lead electrodeposition from 0.50 M Pb $(NO_3)_2$ in 2.0 M $NaNO_3$

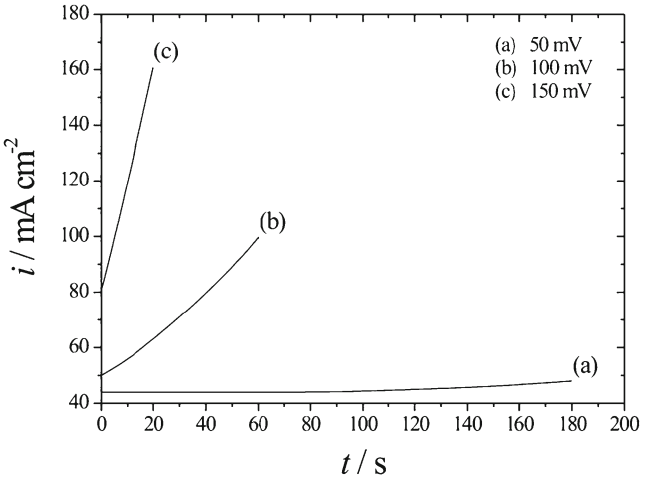

Fig. 2 The dependencies of the current density on electrolysis time obtained for lead electrodeposition at overpotentials of 50, 100, and 150 mV

controlled electrodeposition and in the zone of rapid increase of the electrodeposition current are shown in Figs. 3, 4, and 5, respectively.

Single lead crystals were obtained in the ohmic-controlled electrodeposition at an overpotential of 50 mV (Fig. 3). The formation of these single crystals was accompanied by a small increase in the current during the electrodeposition process. Figure 4 shows that a mixture of different regular geometric forms of lead crystals was obtained at an overpotential of 100 mV, corresponding to the inflection point. The formation of these morphological forms was accompanied by an increase of the electrodeposition current of about 100% in relation to the initial electrodeposition current. Finally, an increase of the current during electrodeposition processes to overpotentials higher than 100 mV was very quick and two-dimensional (2D) single dendrites, as well as those constructed from stalk and primary branches were dominant morphological forms obtained at 150 mV after a two-times increase of the current in relation to the initial electrodeposition current (Fig. 5).

To better clarify the formed morphological forms (especially those obtained at an overpotential of 100 mV), these lead deposits were compared with those obtained in galvanostatic regimes. In the galvanostatic regimes, lead electrodeposition was performed at current densities of 100 and 160 mA/cm^2. These current densities corresponded to the final current densities during electrodeposition in the potentiostatic regimes of electrolysis at overpotentials of 100 and 150 mV, respectively. The lead deposits obtained at current densities of 100 and 160 mA/cm^2 are shown in Figs. 6 and 7, respectively. 2D dendrites were the dominant morphological forms obtained at both current densities. The shape of the 2D dendrites obtained at a current density of 100 mA/cm^2 clearly indicates that the regular geometric forms obtained at an overpotential of 100 mV (Fig. 4b) represents the precursors of dendrites.

It is necessary to note that the dendrites obtained in the galvanostatic regimes were branchier than those obtained in the potentiostatic regimes. In addition to primary branches, secondary branches were also formed during lead electrodeposition at a current density of 160 mA/cm^2 (Fig. 7b). One of the reasons for this is the fact that during electrodeposition in the galvanostatic regime at a current density of 160 mA/cm^2, the initial overpotential was about 220 mV and an overpotential of about 110 mV was attained after electrodeposition after an electrolysis time of 20 s. A similar situation was also observed during lead electrodeposition at 100 mA/cm^2.

Moreover, it can be clearly seen from Figs. 5, 6, and 7 that the shape of the lead dendrites falls under the classical Wranglen's definition of a dendrite. According to Wranglen [26], dendrites consist of stalk and primary and secondary branches. From the electrochemical point of view, a dendrite is defined as an electrode surface protrusion that grows under activation control, while electrodeposition to the macroelectrode is predominantly under diffusion control [27–30]. For very fast

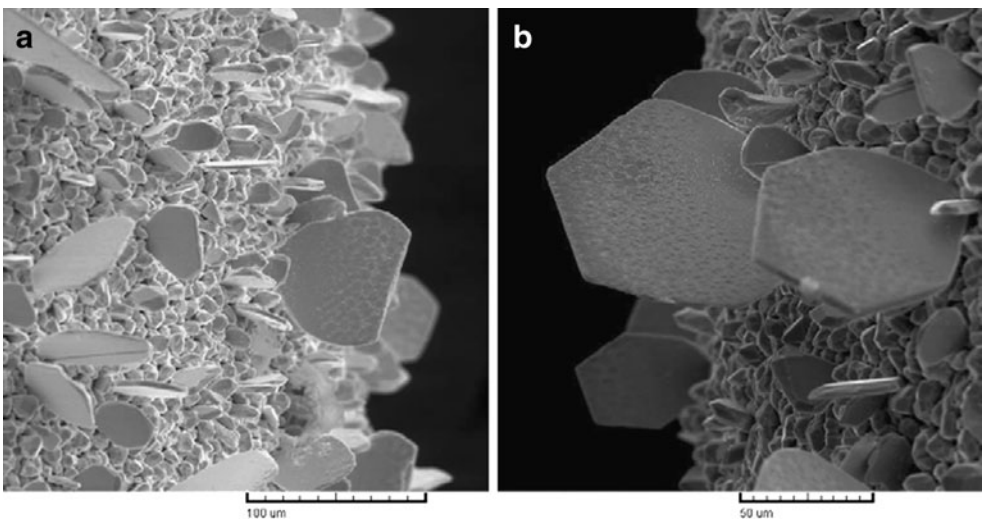

Fig. 3 Lead deposits obtained at an overpotential of 50 mV. Time of electrolysis: 180 s

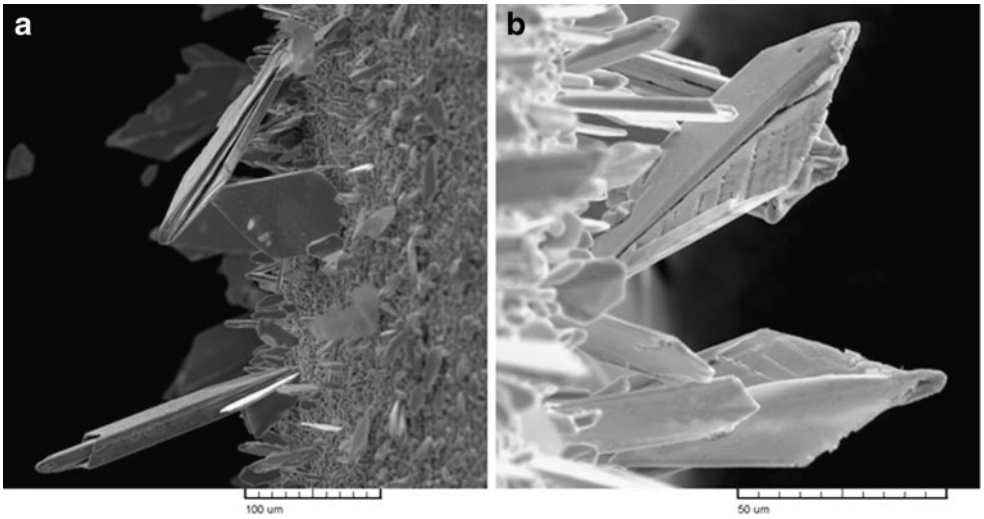

Fig. 4 Lead deposits obtained at an overpotential of 100 mV. Time of electrolysis: 60 s

electrodeposition processes, the critical overpotential for dendritic growth initiation, η_i, and the critical overpotential for instantaneous dendritic growth, η_c, depend on the surface energy of the metal, as presented by Eqs. 1 and 2 [27]:

(a) The critical overpotential for dendritic growth initiation:

$$\eta_i = \frac{8\sigma V}{nF\delta} \tag{1}$$

and

(b) The critical overpotential for instantaneous dendritic growth:

$$\eta_c = \frac{8\sigma V}{nFh}, \tag{2}$$

where V is the molar volume of the deposited metal, σ is the surface energy, which is of the order of a few millivolts [27], nF is the number of Faradays per mole of consumed ions, δ is the diffusion layer thickness, and h is the height of the protrusion.

The initiation of dendritic growth is followed by a strong increase of the apparent current density because the current density at the tips of the formed dendrites is under mixed activation-diffusion or complete activation control. Hence, the strong increase of current with overpotentials higher than 100 mV corresponds to activation controlled electrodeposition on the tips of the formed dendrites. On the other hand, the inflection point, estimated to be at an overpotential of 100 mV, corresponds to the transition from an ohmic to an activation controlled electrodeposition process.

In any case, only two-dimensional forms were obtained during lead electrodeposition. The two-dimensional nucleation was also a characteristic of silver electrodeposition from nitrate solution [31, 32], tin [33], and cadmium electrodeposition [30]. A polarization curve with an inflection point was also obtained in the case of silver electrodeposition from

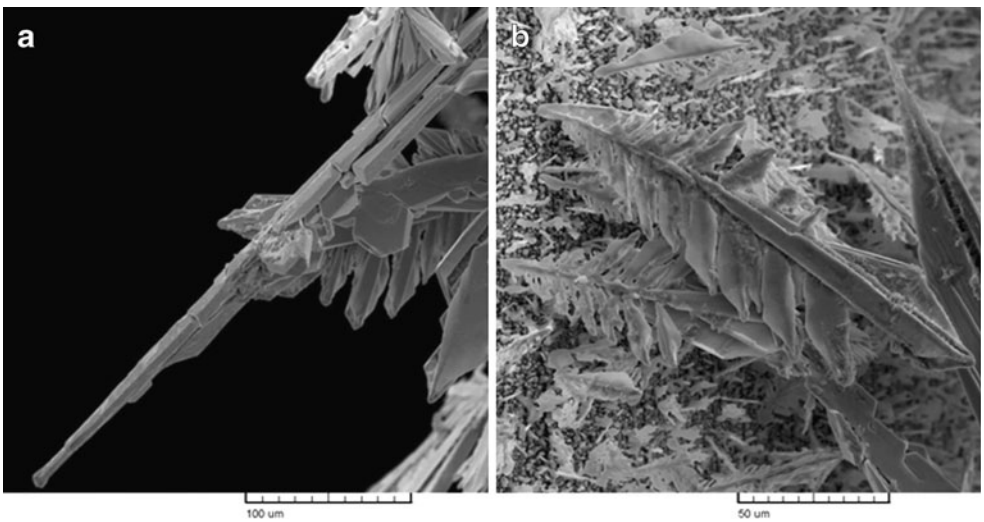

Fig. 5 Lead deposits obtained at an overpotential of 150 mV. Time of electrolysis: 20 s

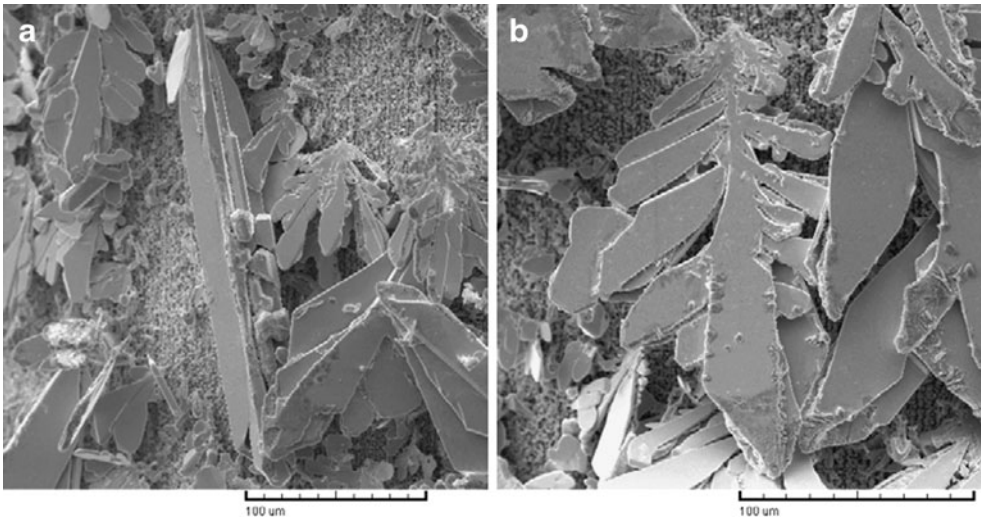

Fig. 6 Lead deposits obtained at a current density of 100 mA/cm^2. Time of electrolysis: 60 s

nitrate solution when a strong increase of current density was accompanied by the formation of dendrites [23, 24], as well as in tin electrodeposition [33]. The common characteristic of these metal electrodeposition processes is their affiliation to the same group of metals, i.e., to the group of normal metals (Cd, Zn, Pb, Sn, Ag (silver nitrate solutions)) [34], which are characterized by a low melting point, T_m, and a high exchange current density, i_0. The shape of the dendrites of this group of metals was completely different from dendrites of copper, which belongs to the second group of metals (intermediate metals, such as Au, Cu, Ag (silver ammonia complex), which are characterized by a moderate T_m and medium i_0). Very branchy 3D (three-dimensional) copper dendrites constructed from corncob-like elements were formed by the processes of electrochemical deposition [35–37]. This indicates a strong dependence of the type of nucleation and the shape of the formed morphological forms on the nature of the metals, which will be examined in more detail in future investigations.

Conclusions

The polarization curve for lead electrodeposition consisted of two parts separated by an inflection point at an overpotential of about 100 mV. The first part of the polarization curve was characterized by a linear dependence of the current density on overpotential (an ohmic-controlled electrodeposition process). The single crystals were formed in the ohmic-controlled electrodeposition.

The second part was characterized by a rapid growth of the current density with increasing overpotential after the inflection point. Two-dimensional (2D) single dendrites, as well as branchy 2D dendrites constructed from primary and secondary branches were formed at overpotentials and the current densities after the inflection point on the polarization curve. Based on the obtained surface morphology, it is concluded that the rapid increase of current after the inflection point can be ascribed to the activation control at the tips of the formed dendrites.

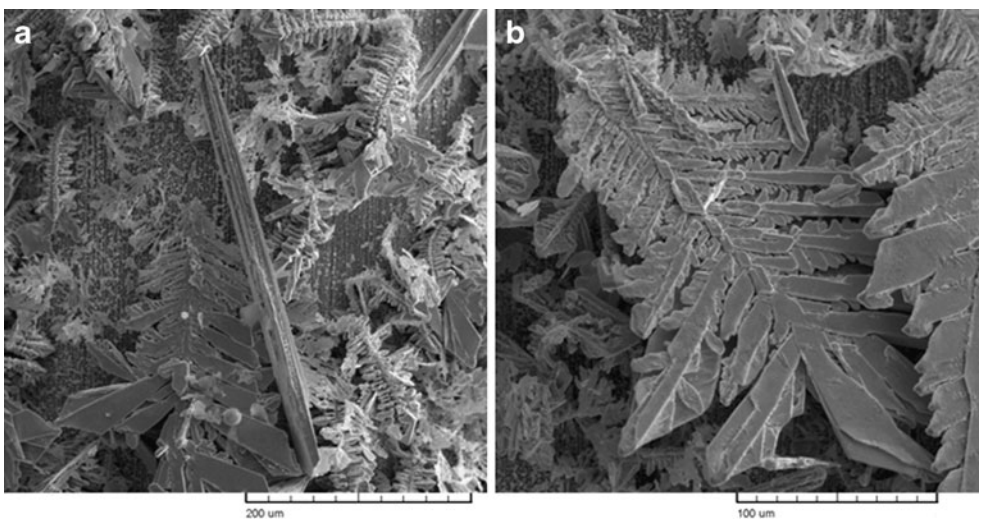

Fig. 7 Lead deposits obtained at a current density of 160 mA/cm^2. Time of electrolysis: 20 s

The morphologies of the obtained lead deposits were compared with those of electrodeposited metals from the same group (normal metals; metals characterized by a high exchange current density), and it was found that the shape of the obtained morphological forms is closely associated with the nature of the metal.

Acknowledgment The authors are grateful to Prof. Dr. Konstantin I. Popov for helpful discussion during the preparation of this paper. The work was supported by the Ministry of Education and Science of the Republic of Serbia under the research project: "Electrochemical synthesis and characterization of nanostructured functional materials for application in new technologies" (no. 172046).

References

1. Pavlov D (1993) Premature capacity loss (PCL) of the positive lead/acid battery plate: a new concept to describe the phenomenon. J Power Sourc 42:345–363
2. Rashkova B, Guel B, Potzschke RT, Staikov G, Lorenz WJ (1998) Electrodeposition of Pb on n-Si(111). Electrochim Acta 43:3021–3028
3. Ehlers C, Konig U, Staikov G, Schultze JW (2002) Role of surface states in electrodeposition of Pb on *n*-Ge(111). Electrochim Acta 47:379–385
4. Avellaneda CO, Napolitano MA, Kaibara EK, Bulhoes LOS (2005) Electrodeposition of lead on ITO electrode: influence of copper as an additive. Electrochim Acta 50:1317–1321
5. Doulakas L, Novy K, Stucki S, Comninellis Ch (2000) Recovery of Cu, Pb, Cd and Zn from synthetic mixture by selective electrodeposition in chloride solution. Electrochim Acta 46:349–356
6. Scharifker B, Hills G (1983) Theoretical and experimental studies of multiple nucleation. Electrochim Acta 28:879–889
7. Mostany J, Parra J, Scharifker BR (1986) The nucleation of lead from halide-containing solutions. J Appl Electrochem 16:333–338
8. Popov KI, Krstajić NV, Pantelić RM, Popov SR (1985) Dendritic electocrystallizaion of lead from lead nitrate solution. Surf Tech 26:177–183
9. Exposito E, Gonzalez-Garcıa J, Bonete P, Montiel V, Aldaz A (2000) Lead electrowinning in a fluoborate medium. Use of hydrogen diffusion anodes. J Power Sourc 87:137–143
10. Popov KI, Stojilković ER, Radmilović V, Pavlović MG (1997) Morphology of lead dendrites electrodeposited by square-wave pulsating overpotential. Powder Technol 93:55–61
11. Ghergari L, Oniciu L, Muresan L, Pantea A, Topan VA, Ghertoiu D (1991) Effect of additives on the morphology of lead electrodeposits. J Electroanal Chem 313:303–311
12. Muresan L, Oniciu L, Froment M, Maurin G (1992) Inhibition of lead electrocrystallization by organic additives. Electrochim Acta 37:2249–2254
13. Muresan L, Oniciu L, Wiart R (1993) On the kinetics of lead electrodeposition in fluorosilicate electrolyte Part I: inhibiting effect of sodium lignin sulphonate. J Appl Electrochem 23:66–71
14. Muresan L, Oniciu L, Wiart R (1994) Kinetics of lead deposition in fluorosilicate electrolyte Part II: inhibiting effect of horse-chestnut extract (HCE) and of sodium lignin sulphonate-HCE mixtures. J Appl Electrochem 24:332–336
15. Carlos IA, Malaquias MA, Oizumi MM, Matsuo TT (2001) Study of the influence of glycerol on the cathodic process of lead electrodeposition and on its morphology. J Power Sourc 92:56–64
16. Wong SM, Abrantes LM (2005) Lead electrodeposition from very alkaline media. Electrochim Acta 51:619–626
17. Carlos IA, Siqueira JLP, Finazzi GA, de Almeida MRH (2003) Voltammetric study of lead electrodeposition in the presence of sorbitol and morphological characterization. J Power Sourc 117:179–186
18. Ghali E, Girgis M (1985) Electrodeposition of lead from aqueous acetate and chloride solutions. Metall Mater Trans B 16:489–496
19. Calusaru R (1979) Electrodeposition of metal powders. Elsevier, Amsterdam, p 351
20. Pavlović MG, Hadžismajlović DžE, Toperić BV, Popov KI (1992) Electrochemical deposition on lead powder by reversing current. J Serb Chem Soc 57:687–696
21. Cherevko S, Xing X, Chung C-H (2011) Hydrogen template assisted electrodeposition of sub-micrometer wires composing honeycomb-like porous Pb films. Appl Surf Sci 257:8054–8061
22. Vijh AK, Randin JP (1977) Some factors determining the rates of electrochemical dissolution-deposition reactions on metallic surfaces. Surf Tech 5:257–269
23. Popov KI, Živković PM, Krstić SB, Nikolić ND (2009) Polarization curves in the ohmic controlled electrodeposition of metals. Electrochim Acta 54:2924–2931
24. Popov KI, Živković PM, Nikolić ND (2010) The effect of morphology of activated electrodes on their electrochemical activity. In: Djokić SS (ed) Electrodeposition: theory and practice, series: modern aspects of electrochemistry, vol 48. Springer, Heidelberg, pp 163–213
25. Bockris JO'M, Reddy AKN, Gamboa-Aldeco M (2000) Modern electrochemistry 2A, fundamentals of electrodics, 2nd edn. Kluwer Academic/Plenum Publishers, New York, p 1107
26. Wranglen G (1960) Dendrites and growth layers in the electrocrystallization of metals. Electrochim Acta 2:130–146
27. Popov KI, Djokić SS, Grgur BN (2002) Fundamental aspects of electrometallurgy. Kluwer Academic/Plenum Publishers, New York, pp 78–89
28. Despić AR, Popov KI (1972) Transport controlled deposition and dissolution of metals. In: Conway BE, Bockris JO'M (eds) Modern aspects of electrochemistry, vol 7. Plenum, New York, pp 199–313
29. Diggle JW, Despić AR, Bockris JO'M (1969) The mechanism of the dendritic electrocrystallization of zinc. J Electrochem Soc 116:1503–1514
30. Popov KI, Krstajić NV, Cekerevac MI (1996) The mechanism of formation of coarse and disperse electrodeposits. In: White RE, Conway BE, Bockris JO'M (eds) Modern aspects of electrochemistry, vol 30. Plenum, New York, pp 261–312
31. Popov KI, Pavlović MG, Stojilković ER, Radmilović V (1996) Silver powder electrodeposition by constant and pulsating overpotential. J Serb Chem Soc 61:47–55
32. Maksimović VM, Pavlović MG, Pavlović LjJ, Tomić MV, Jović VD (2007) Morphology and growth of electrodeposited silver powder particles. Hydrometallurgy 86:22–26
33. Popov KI, Pavlović MG, Jovićević JN (1989) Morphology of tin powder particles obtained in electrodeposition on copper cathode by constant and square-wave pulsating overpotential from Sn(II) alkaline solution. Hydrometallurgy 23:127–137
34. Cherevko S, Chung C-H (2011) Direct electrodeposition of nanoporous gold with controlled multimodal pore size distribution. Electrochem Commun 13:16–19
35. Nikolić ND, Popov KI, Pavlović LjJ, Pavlović MG (2007) Determination of critical conditions for the formation of electrodeposited copper structures suitable for electrodes in electrochemical devices. Sensors 7:1–15
36. Nikolić ND, Pavlović LjJ, Pavlović MG, Popov KI (2008) Morphologies of electrochemically formed copper powder particles and their dependence on the quantity of evolved hydrogen. Powder Technol 185:195–201
37. Nikolić ND, Popov KI (2010) Hydrogen co-deposition effects on the structure of electrodeposited copper. In: Djokić SS (eds) Electrodeposition: theory and practice, series: modern aspects of electrochemistry, vol 48. Springer, Heidelberg, pp 1–70